Optimization of Graphene Oxide Layer Thickness of ZnO-Based Hybrid Solar Cell Using SCAPS 1D: A Comparative Study on ZnO/GO and ZnO/SiO_2 Hybrid Cells

Sakshi Tyagi, Pawan Kumar Singh, and Arun Kumar Tiwari

Abstract In this paper, simulative investigation of a fabricated ZnO/GO hybrid solar cell has been performed using SCAPS 1D software, and it is the one-dimensional solar cell capacitance simulator, widely used for analysis. We have investigated the repercussions of graphene oxide layer thickness on J_{sc} (current density), V_{oc} (open-circuit voltage), FF (fill factor), PCE (power conversion efficiency of the cell). A comparison was made between the simulated data and experimental data based on experimentation. It has been observed that V_{oc} and FF of simulation and experimental analysis show a good agreement. But J_{sc} is on a higher end for simulated results compared to experimental result, which is due to graphene layer thickness imperfection and absorption. Further, performance of ZnO/GO cell was compared to ZnO/SiO_2 cell and it was found that the efficiency of the two is nearly similar when evaluated at 32^0 C under 1 Sun and AM 1.5. A limiting factor in using the high-efficiency Si homojunction solar cell is its high fabrication cost. Hence, here we try to replace GO with SiO_2 because of its simpler synthesis and involved fabrication processes. But the only backdrop is its lower efficiency, which can be improved by simulation analysis discussed in this work. This work presents the results which can improve the performance of graphene-based solar cells by simulation, increasing the efficiency, reducing the overall manufacturing cost and hence proves to be an asset to the society.

Keywords Synthesis · Simulation · SCAPS 1D

S. Tyagi (✉) · P. K. Singh
Department of Mechanical Engineering, Indian Institute of Technology (ISM), Dhanbad, Jharkhand 826004, India
e-mail: tyagi.sakshi615.hcst@gmail.com

A. K. Tiwari
Department of Mechanical Engineering, Institute of Engineering and Technology, Lucknow, Uttar Pradesh 226021, India

V. Mahajan et al. (eds.), *Sustainable Technology and Advanced Computing in Electrical Engineering*, Lecture Notes in Electrical Engineering 939,
https://doi.org/10.1007/978-981-19-4364-5_56

1 Introduction

The depletion of natural resources, considerable increase in energy demands and other environmental issues are the major reasons for many countries to prioritize the evolution of renewable energy resources. Nowadays, sustainable energy is one of the vital resolutions to encounter the energy demands of the upcoming era. It can be used as an eco-efficient substitute to fossil fuels and possesses a huge benefit of being clean, green and toxin-free. Solar energy is considered to be one of the best renewable energy sources that proved to be a marvellous substitute to fossil fuels because of its low cost, easy availability and environment-friendly nature. Nowadays, modelling and simulation of photovoltaic cells have achieved enormous heed in various areas. There has been the development of innovative methods for manufacturing and improving the efficiency of the solar cells. The next generation of solar cells involves development of hybrid cells, which are evolved by combination of inorganic and organic semiconductors which are certainly accessible in the nature and are harmless too. In this present scenario of pandemic, where the world is surviving hard, renewable energy sector has also suffered a steep reduction in manufacturing phase. Energy demands have soared high in the last few years, but the sector is facing unreliability to meet the demands with inappropriate resources, high manufacturing and fabrication price. Hence to maintain sustainable energy requirements, simulation of hybrid solar cells has emerged as an efficient substitute to the expensive PV cells. The presented work shows the simulation of ZnO/GO cell by implementing solar cell capacitance simulator (SCAPS 1D) software. ZnO has been used because of its ability of sustaining high temperatures and its large bandgaps. High absorption coefficient, abundant availability and acceptable sensitivity in UV region make it a useful candidate for application in thin-film solar cells. Graphene has also presented good results in solar cell applications. The discipline of hybrid devices has matured by adding of graphene layer in the device structure, hence making it more worthy. Current research has presented the use of graphene-based transparent electrodes for hybrid solar cells where graphene oxide/ZnO was used in the front contact on ITO [1]. Perovskite cells still have several drawbacks like UV and heat decomposition instability at moisture and ion electromigration. Graphene derivatives combat the following problems and prove to be a suitable candidate for inclusion in hybrid solar cell. Some authors have also discussed a reduced form of graphene oxide (r-GO)/CuSCN which acts as efficient bilayer hole transport layer (HTL) [2]. Numerous simulation analyses have already been performed on enhancing the stability and efficiency of nanotube and graphene contacted solar cells (CdTe, CIGS, CZTS, perovskites) [3, 4].

This research work aims to determine the possible chances of integrating zinc oxide along with graphene oxide layer in the proposed cell structure. The evidences obtained for such structures have been discussed here. SCAPS 1D software 3.3.08 version has been used as a platform for simulation of mentioned cell structure, and the results were compared to the experimental results. The synthesis and fabrication process of ZnO/GO hybrid cell along with device structure and simulation procedure are discussed. Effect of graphene oxide layer thickness on the various photovoltaic

parameters of cell is studied. Performance graphs of ZnO/GO and ZnO/SiO_2 solar cell are evaluated. Literature has not reported any research on the discussed pair of cells using the software SCAPS 1D. Further, this study is useful in modelling and simulation of hybrid solar devices which are useful in many solar polygeneration systems.

2 Experimental

2.1 Synthesis and Fabrication of ZnO/GO Cell

Synthesis of zinc oxide was done using ethanol, sodium hydroxide and zinc nitrate, purchased from Sigma-Aldrich. Nanoparticle synthesis was done using wet chemical technique. Aqueous ethanol solution of zinc nitrate (Zn(NO3)2·4H2O) brought in use was 0.5 M. Then continuous stirring with the help of magnetic stirrer was performed over the solution. After an hour, zinc nitrate was dissolved. Similarly, 0.8 M aqueous ethanol suspension of potassium hydroxide (KOH) was composed and stirred for an hour maintaining a speed of 320–340 RPM [5]. On complete dissolving of zinc nitrate, 0.8 M KOH aqueous suspension was introduced drop by dropwise for 45 min. After mixing all the products, we set the seal onto the flask boundaries in order to permit the reaction to commence for 3 h. On completion of the reaction, the suspension was kept for overnight and then segregation is done [6]. The precipitate was separated from left over solution which was centrifuged for 15 min. Now washing of the precipitated NPs of ZnO with ethanol and deionized water and was performed three times to remove the by-products. Air drying at 60 °C in is performed for the precipitate. Now by desiccation, $Zn(OH)_2$ is entirely converted to ZnO, Fig. 1. SEM images of the ZnO NPs have been studied here for further investigation.

2.2 Synthesis of Graphene Oxide

Pure graphite particles with a purity of 99.8% and −325 mesh size were purchased from Hemadri Chemicals, Mumbai. The developments for processing of GO were done using modified Hummers' method. The measure of graphite particles and $NaNO_3$ used in the process was 5.5 g and 3.5 g, respectively. Now 12 ml H_3PO_4 and 108 ml H_2SO_4 were mixed to it, and the solution was kept under constant stirring for 15 min in an ice bath. The suspension temperature was kept below 50 °C, and then 15 g of $KMnO_4$ was slowly added to it. Then in an ice bath, the suspension was reacted for 2.5 h. Water was added continuously for 70 minutes to maintain a temperature of 98 °C. The solution volume was increased upto 500 ml by adding deionized water to it [7]. Then 15 ml of H_2O_2 was added after a gap of 15 mins. The product so obtained was centrifuged with 5% HCL and was dried at 60 °C, refer to Fig. 1.

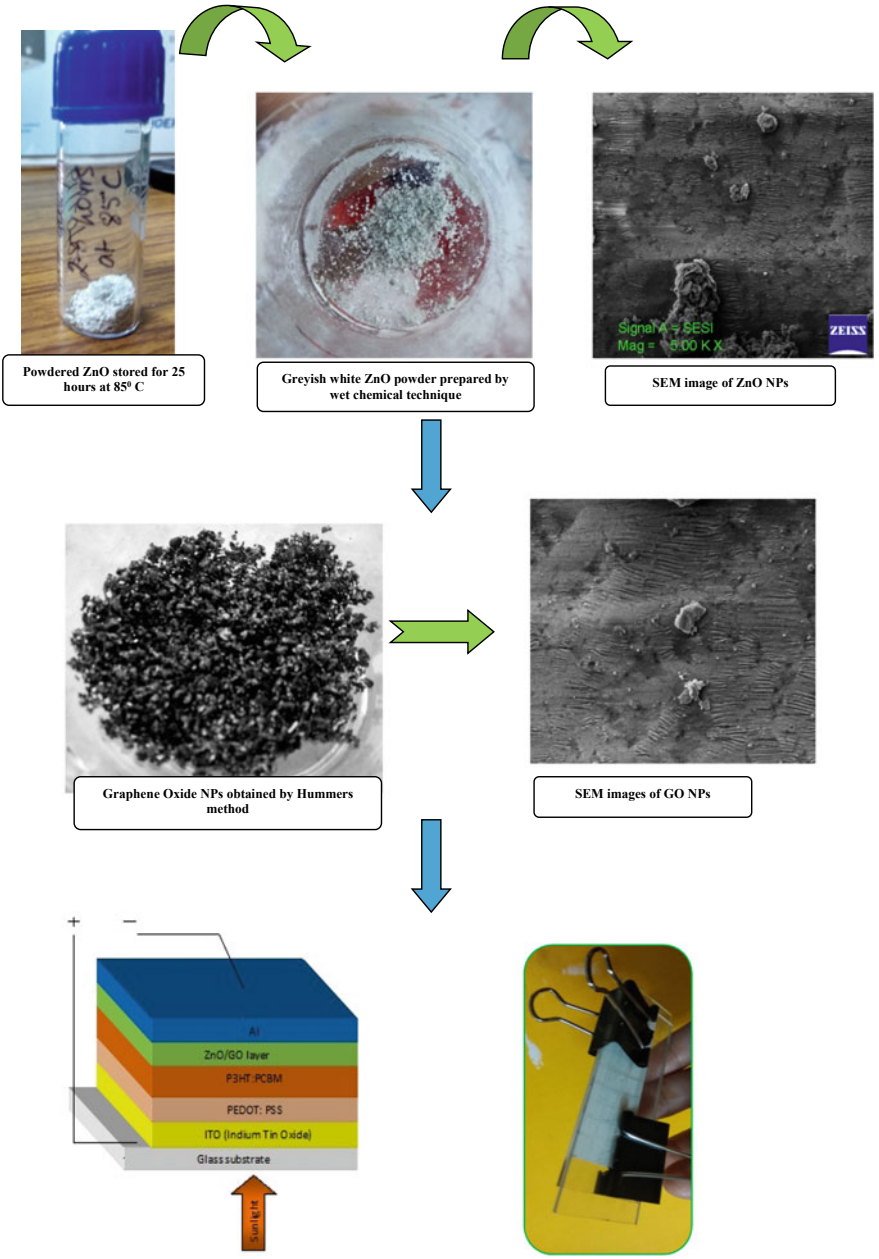

Fig. 1 Device structure of ZnO/GO hybrid solar cell and fabricated ZnO/GO cell

3 Device Structure and Simulation Method

SCAPS-1D software also known as solar cell capacitance simulator was developed at the Department of Electronics and Information Systems (EIS), University of Ghent, Belgium. Being single-dimensional simulation software, it is basically utilized for numerical analysis of solar cells [6, 8]. The present work reveals the numerical simulation performed on ZnO/GO hybrid solar cell using SCAPS-1D version 3.3.08 to analyse the performance of graphene oxide layer on the overall device performance. Also, photovoltaic parameters such as V_{oc}, J_{sc}, FF and power conversion efficiency were obtained from simulated results.

The schematic device structure of the ZnO/GO solar cell which has been adopted in this study is presented in Fig. 1. It comprises of transparent ITO glass substrate, where a layer of PEDOT:PSS of 5.0 eV work function is spread upon it for electron collection. ZnO/GO plays the role of electron transport layer and photoactive layer, respectively. P3HT:PCBM layer helps in photon electron conversion and is a good acceptor too. On the top, aluminium electrode is inserted. By this simulation, photovoltaic parameters (J_{sc}, V_{oc}, FF and PCE) of the ZnO/GO hybrid solar cell were obtained and then compared to the experimental results [6]. The selection of parameters was done used on the basis of the experimental and theoretical results; also, reasonable estimation has been performed, in Table 1. Here, for all the simulations, temperature of 27 °C, illumination values of 1000 W/m^2 and air mass of 1.5 G have been considered. Also, a precise comparison has been made between the PV characteristics of ZnO/GO and ZnO/SiO_2 cells.

4 Results and Discussion

4.1 Effect of Graphene Oxide Layer Thickness

The device structure of ZnO/GO hybrid solar cell illustrated in Fig. 1 was analysed in SCAPS 1D platform and the experimental results and literature helped in fetching the device parameters for the cells. The experimental results of the device have been presented in Table 1, and the device characteristics like short-circuit current density, power conversion efficiency, fill factor and open-circuit voltage have been reported here under 1.5 A and 1 sun [9]. However, simulation of the IV characteristics of the cell has been performed by placing appropriate values to the variables of the device layers. Furthermore, we have compared the PV characteristics like fill factor (FF), short-circuit current density (J_{sc}), open-circuit voltage (V_{oc}), PCE of ZnO/GO by experimental and simulation analysis. Also, comparison is drawn between characteristics of ZnO/GO and ZnO/SiO_2 cells. By incorporation of graphene layer in such devices, there is considerable reduction in ion electromigration from metallic electrode to ZnO layer along with improvement in the carrier collection at top electrode [10–12]. During actual operation, rise in the heat dissipation from the

Table 1 Extracted parameters of ZnO/GO solar cell

		Control parameters		Responses			
	Data	Spectral power density (W m^{-2})	Temperature (K)	Open-circuit voltage (V_{oc}) V	Current density (J_{SC}) (mA/cm^2)	Fill factor (%)	Power conversion efficiency (PCE) %
Day 1	1	1006.6	305.6	0.69	6.89	56.62	8.96
	2	1005.7	305.1	0.62	7.24	56.94	9.12
	3	1005.5	305.7	0.74	6.77	56.87	8.42
	4	1008.2	306.4	0.72	6.49	56.22	8.64
	5	1006.4	304.3	0.71	6.58	56.87	9.07
	6	1009.6	302.4	0.68	7.17	54.12	8.45
	7	1007.1	305.6	0.69	7.24	52.91	8.66
	8	1005.6	306.4	0.68	7.13	51.78	8.52
	9	1004.5	304.7	0.64	7.51	54.76	8.49
	10	1006.4	306.4	0.63	7.11	53.85	9.12
	11	1008.6	302.5	0.69	6.66	54.72	8.46
	12	1007.8	304.8	0.72	6.85	55.74	8.62
	13	1005.8	306.9	0.68	6.94	56.92	8.44
	14	1006.4	303.4	0.64	6.96	56.84	8.38
	15	1005.1	305.9	0.72	7.24	52.19	8.52
	16	1006.2	303.2	0.69	7.24	51.27	8.46
	17	1009.6	306.6	0.63	7.17	54.71	8.39
	18	1007.4	306.4	0.72	6.28	56.78	9.08
	19	1008.6	302.8	0.65	6.44	57.83	9.07
	20	1007.5	301.7	0.68	6.84	56.87	9.12
	21	1006.2	301.2	0.66	6.11	56.22	9.08
	22	1009.7	308.9	0.65	6.47	56.87	9.12
	23	1008.1	306.8	0.64	6.82	54.12	9.12
	24	1005.5	307.2	0.72	7.17	52.91	9.04
	25	1008.3	309.3	0.78	7.24	51.78	8.56
	26	1009.2	304.6	0.72	7.13	54.76	8.97
	27	1006.7	301.2	0.74	7.51	53.85	8.67
	28	1007.4	307.5	0.68	7.11	54.72	8.29
	29	1005.4	307.4	0.65	6.66	55.74	8.38
	30	1006.8	309.8	0.64	6.85	56.92	8.52
	31	1005.9	304.7	0.68	7.17	56.84	8.46
	32	1006.2	306.7	0.68	7.24	52.19	8.39
	33	1006.3	307.9	0.64	7.24	51.27	9.08

(continued)

Table 1 (continued)

		Control parameters		Responses			
	Data	Spectral power density (W m^{-2})	Temperature (K)	Open-circuit voltage (V_{oc}) V	Current density (J_{SC}) (mA/cm^2)	Fill factor (%)	Power conversion efficiency (PCE) %
	34	1008.4	308.2	0.64	7.17	54.71	9.07
	35	1009.8	307.7	0.62	6.28	56.78	9.12
	36	1006.8	308.4	0.69	6.44	57.83	9.08
	37	1008.6	305.5	0.72	6.84	56.62	9.12
	38	1009.9	307.8	0.72	6.11	56.94	9.12
	39	1007.6	304.6	0.64	6.47	56.87	9.04
	40	1005.6	304.7	0.67	6.77	56.22	8.56
	41	1006.7	307.7	0.64	6.49	56.87	8.97
	42	1008.4	302.8	0.66	6.58	54.12	8.67
	43	1007.6	304.8	0.64	7.17	52.91	8.29
	44	1007.4	301.7	0.68	7.24	51.78	8.38
	45	1008.2	305.4	0.65	7.13	54.76	8.52
	46	1009.6	305.6	0.62	6.77	53.85	8.46
	47	1007.8	307.8	0.67	6.49	54.72	8.39
	48	1006.2	302.8	0.68	7.24	55.74	9.08
	49	1005.4	301.2	0.62	7.24	56.92	9.07
	50	1006.1	301.4	0.67	7.17	56.84	9.12
	51	1006.7	302.5	0.72	6.28	52.19	9.08
	52	1007.7	305.6	071	6.44	51.27	9.12
	53	1007.8	302.7	0.72	6.84	54.71	9.12
	54	1005.6	305.6	0.65	6.11	56.78	9.04
	55	1006.1	307.2	0.70	6.47	57.83	8.56
	56	1005.4	302.8	0.72	6.82	56.87	8.97
	57	1006.7	307.2	0.71	7.24	56.22	8.67
	58	1008.4	306.4	0.72	7.24	56.87	8.29
	59	1009.4	304.7	0.71	7.17	54.12	8.38
	60	1007.8	305.8	0.72	6.47	52.19	8.52
	61	1008.8	304.7	0.69	6.77	51.27	8.46
	62	1009.7	301.3	0.68	6.49	54.71	8.39
	63	1007.8	304.6	0.72	6.58	56.78	9.08
	64	1008.8	305.7	0.71	7.17	57.83	9.07
	65	1007.5	302.8	0.72	7.24	56.87	9.12

(continued)

Table 1 (continued)

		Control parameters		Responses			
	Data	Spectral power density (W m^{-2})	Temperature (K)	Open-circuit voltage (V_{oc}) V	Current density (J_{SC}) (mA/cm^2)	Fill factor (%)	Power conversion efficiency (PCE) %
	66	1006.7	308.5	0.71	7.13	56.22	9.12
	67	1005.9	304.9	0.70	6.77	56.87	9.04
	68	1005.8	302.9	0.71	6.49	52.19	8.56
	69	1005.9	309.2	0.72	7.24	51.27	8.97
	70	1006.8	304.9	0.72	6.28	54.71	8.67
	71	1009.2	304.8	0.72	6.44	54.76	8.29
	72	1005.2	308.4	0.68	6.84	53.85	8.38
	73	1006.4	301.4	0.68	6.11	54.72	8.52
	74	1008.2	303.5	0.66	6.47	55.74	8.46
	75	1007.8	308.4	0.68	6.82	56.92	8.39
	76	1006.2	309.7	0.66	7.17	56.84	9.08
Day 16	77	1008.8	302.7	0.69	7.24	52.19	9.07
	78	1006.7	302.9	0.66	7.13	51.27	9.12
	79	1009.5	304.9	0.71	7.51	54.71	9.12
	80	1008.9	308.7	0.72	7.11	56.78	9.04

graphene layer to the environment increases the thermal stability of cell; also, there is a reduction in the heat generated within the cell [13]. As suggested in several papers, graphene layer was considered as a planar structure. For this research, GO is considered as a planar layer with p type doping of up to 50 nm thickness.

4.2 Comparative Study on Experimental and Simulated Results for ZnO/GO Cell

The efficacy of solar cells is dependent on the extracted variables, i.e. short-circuit current density J_{sc}, the open-circuit voltage V_{oc} and the fill factor FF which eventually helps in deciding the power conversion efficiency of the device. The solar cell was positioned under the sun for 16 days for 7 hours daily. For each day, 5 readings were obtained, and the results were noted after every 150 min. The notable values of current are determined for the mentioned device on availability of solar energy. An ammeter and multimeter are used to measure the short-circuit current and voltage, respectively, for the solar cells. With reference to literature, these parameters are determined by examining an illuminated I–V characteristic curve for standard cells [6, 14, 15]. For

correct analysis of the I–V characteristics, it is important to execute the calculations under regular test environment with total irradiance equal to 1000 W/m^2 and 1.5 AM spectrum [16]. Temperature plays pivotal role in the determining the efficacy of a solar cell, which was estimated using thermometer. The mean value of temperature estimated for 16 days for the hybrid device was 33 °C. Hence, depending on the mean value of estimated light intensity of 2612 lx for the cell, the results for spectral power density range from 1005.6 to 1009.4 W/m^2 for 16 days.

The simulated device metrics of the cell designed in SCAPS-1D have been plotted in Fig. 2. Comparable results were obtained by designing the cell and simulative analysis. Both V_{oc} and FF are comparable for the two modes of investigation. However, the simulated value of J_{sc} is on a higher end (12.46 mA/cm^2 vs.7.24 mA/cm^2) than the pilot value. In SCAPS 1D, it is recommended to insert graphene planar layer of appropriate absorption coefficient. The experimental values are almost half of the simulated current–density. The higher value of current density could be due to the thickness of graphene oxide layer (50 nm).

The variables of simulated device have been presented here. Out of simulations, comparable metrics were investigated and few discrepancies were reported as the interface mismatch in the cell. Figure 2 represents the IV characteristic curve for ZnO/GO cell, where a comparable graphical analysis is made in between experimental (real) and simulated (identified) results. Also, graphene has been considered as a planar p type layer in SCAPS-1D simulation. Graphene has opto-electronics

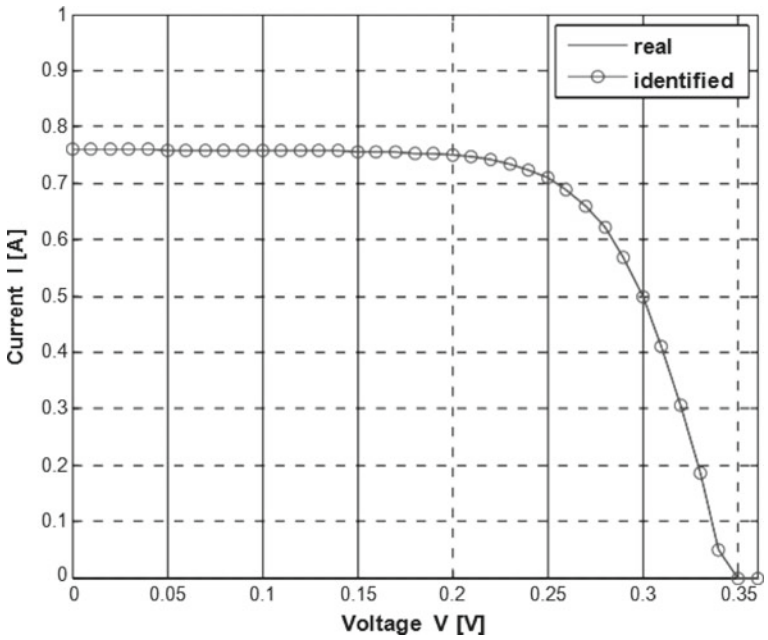

Fig. 2 IV characteristics curve of the ZnO/GO cell, designed in SCAPS-1D

properties which are similar to the p type doped thin metallic layer [16]. It is observed that by increase in graphene thickness, a significant change in the device parameters is noted. Figure 3a–d illustrates the variation of V_{oc}, J_{sc}, FF and PCE by increase in graphene oxide thickness. Also, Fig. 4a–d illustrates the variation of V_{oc}, J_{sc}, FF and PCE by increase in conventional silicon dioxide layer thickness. V_{oc} shows an increase in the beginning and then tends to be constant around 0.78 V for GO thickness (tGO) >37 nm. The reason behind good interface and charge collection at the ZnO/GO layer could be due to the increased number of atomic orbitals of graphene layers [17, 18]. Also, match and interaction of the grid at the interactive boundary will enhance by increase in graphene atomic orbitals. Due to the more number of graphene atoms in the cell structure, there is high lateral resistance in the junction [19–21]. This resulted in sharp decline of fill factor for thickness lesser than 45 nm. When thickness exceeds the mark of 45 nm, FF shows a constant behaviour. In the beginning, J_{sc} has shown a slight odd pattern but then it started increasing for thickness >35 nm. It is expected since we have introduced graphene as a plane and smooth layer in the device framework [22]. Further, if the thickness of this layer is increased, it will increase the absorption rate. The efficiency has shown a decreasing pattern by increased tGO values and gets saturated around 8.46 % for tGO > 47 nm. The decrease in PCE generally follows the reduction in fill factor.

It is observed that for this cell structure, t_{gr} > 30 nm is optimum thickness value for V_{OC} and J_{SC} and t_{gr} > 45 nm is reported as optimal value for FF and PCE.

V_{oc} tends to increase upto a thickness of 34 nm and then becomes constant around 0.82 V for SiO_2 thickness from 30 to 42 nm. There is again an increase in voltage from thickness 45–52 nm. Jsc increases upto 50 nm and then comes around saturation point and follows a constant line for value of 15.52 mA/cm^2. Reduction in fill factor is recorded for thickness upto 45 nm. Then a constant curve is obtained for thickness of SiO_2 between 45 and 52 nm. A decreasing trend in the efficiency is noted around 9.46 % for SiO_2 thickness > 45 nm.

4.3 Performance Comparison of ZnO/GO and ZnO/SiO_2 Cell

To substantiate our work and for understanding the motive for using GO at the upper surface, we reproduced the different parameters like V_{OC}, J_{SC}, FF, PCE of the hybrid solar cell, where GO is replaced with silicon dioxide [23, 24]. The comparable simulation values state that graphene can be a suitable substitute for traditional silicon hole transporting layer in hybrid cells despite a moderately low PCE and fill factor values. It is also stated in many publications that a sensibly incapacitated graphene layer can efficiently work as back contact and hole conduction surface in hybrid solar devices [25–27]. By this comparable result, it is suggested that graphene can be a sensible contacting layer. We have determined good agreement between the experimental and simulation results for silicon dioxide hybrid cell where values of the fill factor, conversion efficiency and voltage are almost similar. Comparative

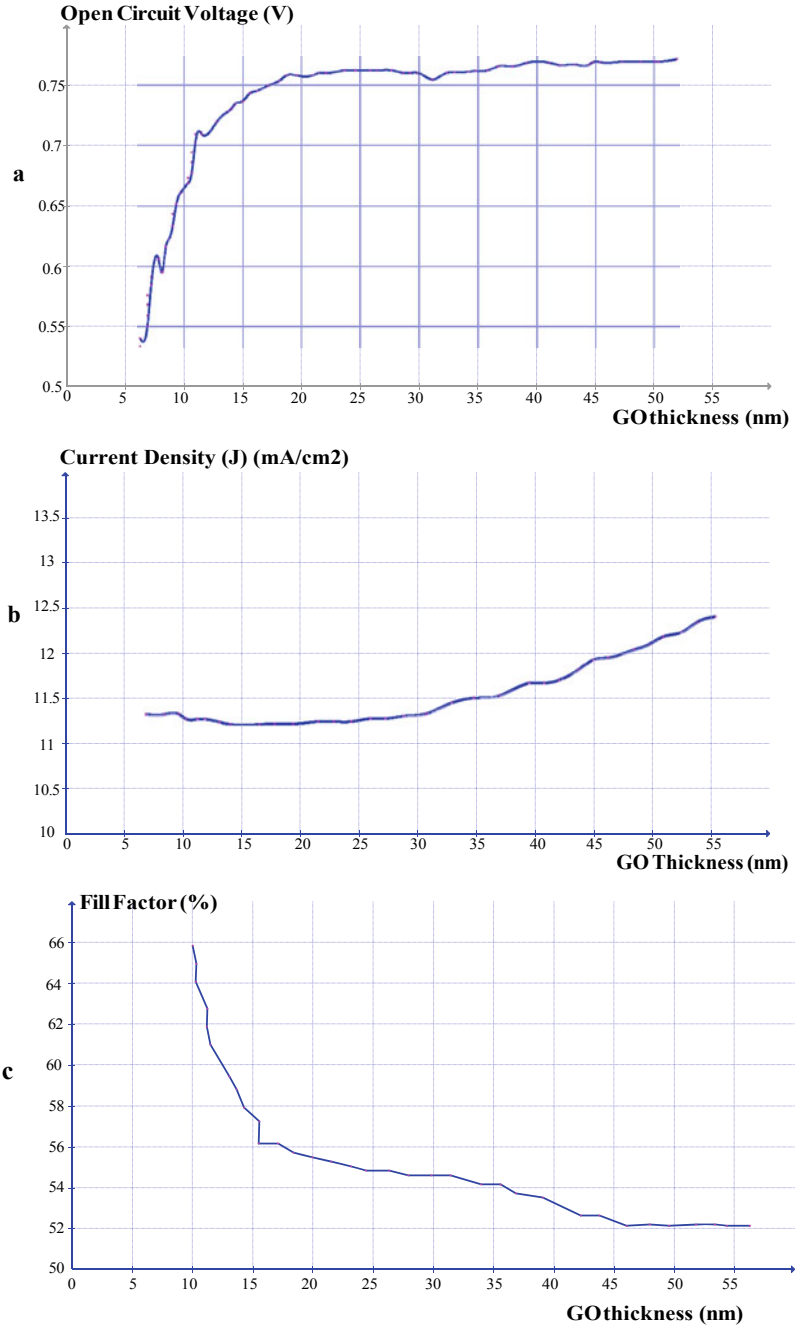

Fig. 3 **a–d** Influence of increased thickness of GO layer on VOC, JSC, FF, PCE of the hybrid solar device drawn in SCAPS-1D

Fig. 3 (continued)

values of simulated and experimental results for both the device structures have been shown in Table 2.

Further, it is observed that on insertion of GO layer, there is increase in JSC in simulation results. It is certainly due to a better photo-absorption and thin thickness [28–30]. We believe that in SCAPS simulation there are no other mechanisms which can explain incorporation of the analytically fabricated cell which is due to multiple reflections from the interfaces and reflection at the back contact [31–33]. Hence, by this examination graphene oxide is again proved to be a promising material to replace SiO_2 for suitable architecture designing of hybrid solar cells.

5 Conclusion

In the present research, numerical simulations were performed for ZnO/GO and ZnO/SiO_2 hybrid solar cell. The result of varied graphene oxide thickness on the photovoltaic parameters was closely studied. An experimental study has been made to determine the device variables of two hybrid solar cells and then the results were compared. We introduced the simulative investigation of the different features of graphene contacted ZnO hybrid solar devices where GO is attached on upper surface and it also acts as hole conducting layer. Similar procedure of comparison of simulated results has been applied and hence we were able to conclude that graphene can be a better candidate to replace the silicon layer in the hybrid cells. This investigation has efficiently resulted in comparable outcomes for current, voltage, fill factor and conversion efficiency. Conversion efficiency of 12.46 % was obtained which can easily be increased by parametric optimization of the cell, essential parameters

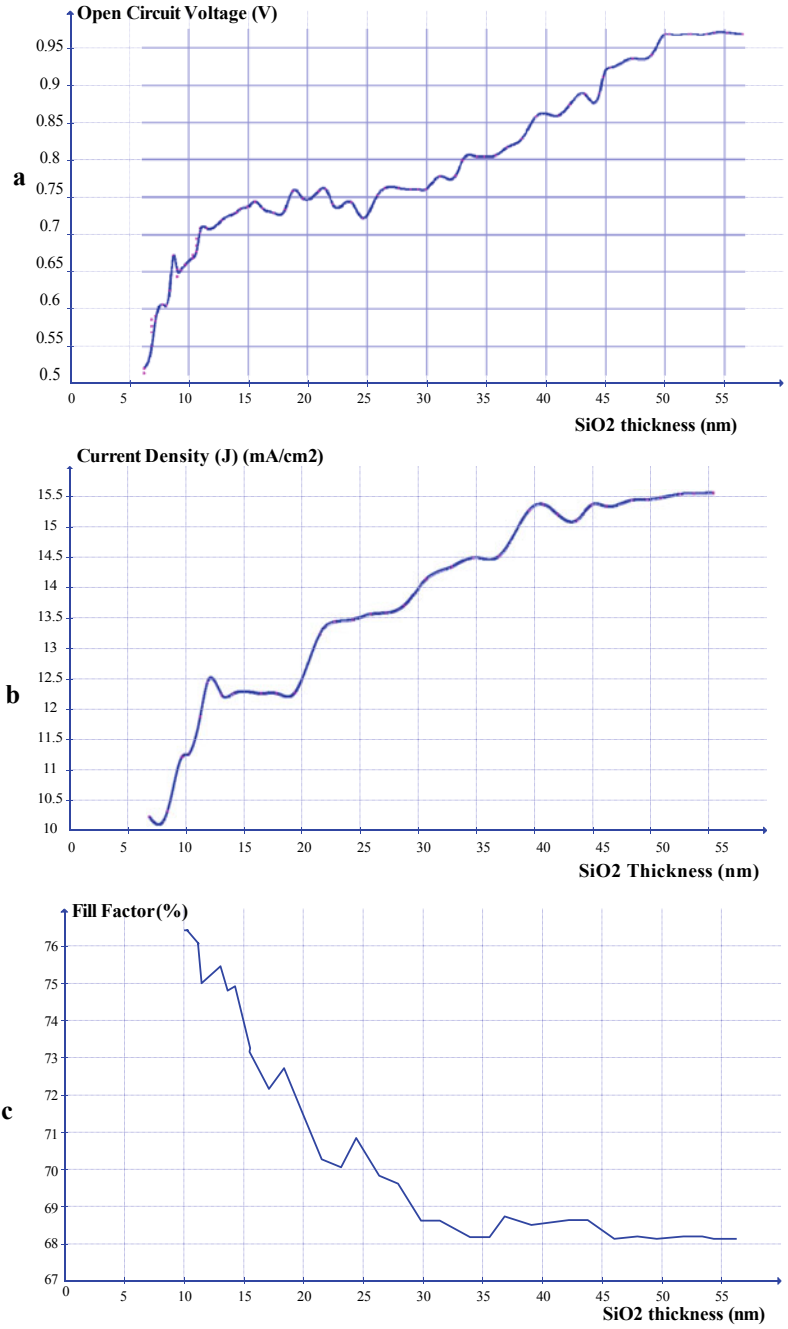

Fig. 4 **a–d** Influence of increased thickness of SiO_2 layer on V_{OC}, J_{SC}, FF, PCE of the hybrid solar device drawn in SCAPS-1D

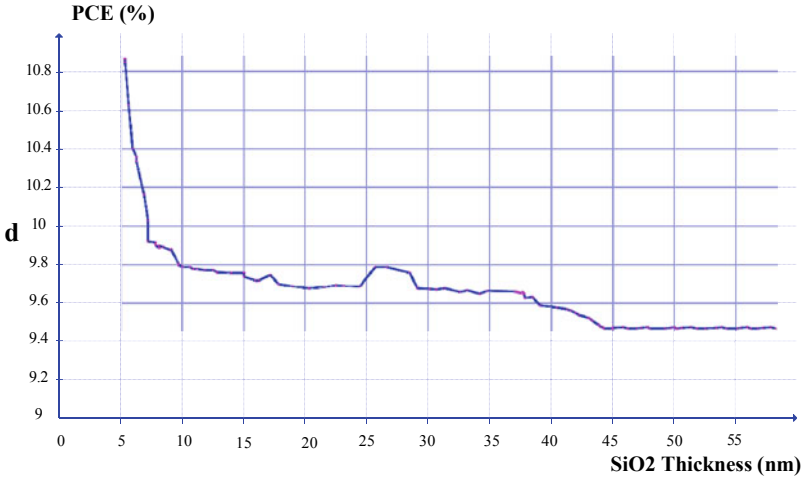

Fig. 4 (continued)

Table 2 Comparison of experimental and simulation analysis

Cell structure	V_{oc}	J_{sc}	FF	PCE
ZnO/SiO_2 (experiment)	0.94	15.74	67.38	10.35
ZnO/SiO_2 (simulation)	0.97	15.52	68.42	9.47
ZnO/GO (experiment)	0.72	7.24	56.94	9.12
ZnO/GO (simulation)	0.79	12.46	52.14	8.46

being doping density and gap of the GO layer. Graphene has been exhibited as a rational substitute for silicon traditional hole transporting layer. However, slightly lower value of fill factor of ZnO/GO can be easily optimized by suitable doping with metallic ions. Favourable thickness seems to be 30nm for which there is increase in Voc and Jsc. The optimum thickness value for FF and PC is 45 nm. It also appears that graphene oxide thickness shall produce lower values of fill factor for thicker layers. At last, comparisons were drawn in between experimental and simulated values for ZnO/GO and ZnO/SiO_2, respectively, and it can be summed up that GO can be efficiently replaced with SiO_2.

Performed work shows the evaluative features which can enhance the device performance of ZnO and GO nanostructured cells, and hence, the research also involves the designing and optimization of similar devices made of carbon nanotubes.

Acknowledgements The authors highly acknowledge and are thankful to Dr. Marc Burgelman at the University of Gent, Belgium for providing SCAPS to perform the simulation analysis.

Declaration of Competing Interest The authors proclaim that they have no known competing financial interests or personal relationships that could have appeared to influence the work reported in this paper.

References

1. Chen Y, Meng Q, Zhang L, Han C, Gao H, Zhang Y, Yan H (2019) SnO_2-based electron transporting layer materials for perovskite solar cells. A review of recent progress. J Energy Chem 35:144–167
2. Chowdhury TH, Akhtaruzzaman M, Kayesha M, Kaneko R (2018) Low temperature processed inverted planar perovskite solar cells by r-GO/CuSCN hole-transport bilayer with improved stability. Sol Energy 171:652–657
3. Milic JV, Arora N, Dar M (2018) Reduced graphene oxide as a stabilizing agent in perovskite solar cells. Adv Mat Interfaces 5:1800416
4. Kang AK, Zandi MH, Gorji NE (2019) Simulation analysis of graphene contacted perovskite solar cells using SCAPS- 1D. Opt Quant Electron 51:91
5. Abbasi HY, Habib A, Tanveer M (2017) Synthesis and characterization of nanostructures of ZnO and ZnO/graphene composites for the application in hybrid solar cells. J Alloys Compd 690:21–26
6. Tyagi S, Singh PK, Tiwari AK, Pain P (2021) Optimization and comparison of photovoltaic parameters of zinc oxide (ZnO)/graphene oxide (GO) and zinc oxide (ZnO)/carbon quantum dots (CQDs) hybrid solar cell using firefly algorithm for application in solar trigeneration system in commercial buildings. Sustain Energy Technol Assess 47:101357
7. Song J, Wang, X, Chang CT (2014) Preparation and characterization of graphene oxide. J Nanomaterials 2014
8. Fonash SJ (1997) A manual for AMPS-1D: a one-dimensional device simulation program for the analysis of microelectronic and photonic structures. The center for nanotechnology education and utilization, The Pennsylvania State University, University Park, PA 16802
9. Jhuma FA, Shaily MZ, Rashid MJ (2019) Towards high-efficiency CZTS solar cell through buffer layer Optimization. Mat Ren Sust Energy 8
10. Kuhn L, Gorji NE (2016) Review on the graphene/nanotube application in thin film solar cells. Mat Letters 171:323–326
11. Iqbal T, Haqnawaz M, Sultan M, Tahir MB (2018) Novel graphene-based transparent electrodes for perovskite solar cells. Int J of Energy Res 42:1–9
12. Yang Y, Xiao J (2014) An all-carbon counter electrode for highly efficient hole- conductor-free organo-metal perovskite solar cells. RSC Adv 4:52825–52830
13. Yoo MJ, Park HB (2019) Effect of hydrogen peroxide on properties of graphene oxide in Hummers method. Carbon 141:515–522
14. Zhang Y, Gao Z, Song N, He J, Li X (2018) Graphene and its derivatives in lithium–sulfur batteries. Mat Today Energy 9:319–335
15. Ghosh S, Harish S, Ohtaki M, Saha BB (2020) Thermoelectric figure of merit enhancement in cement composites with graphene and transition metal oxides. Mat Today Energy 18:100492
16. Talam S, Karumuri SR, Gunnam N (2012) Synthesis characterization and spectroscopic properties of ZnO nanoparticles. Int Sch Res Netw 2012
17. Norton M, GraciaAmillo AM, Galleano R (2015) Comparison of solar spectral irradiance measurements using the average photon energy parameter. Sol Energy 120:337–344
18. Ansari ZA, Singh TJ, Islam SM, Singh S, Mahala P, Khan A, Singh KJ (2019) Photovoltaic solar cells based on graphene/gallium arsenide Schottky junction. Optik Int J for Light and Electron Optics 182:500–506
19. Wang C, Tang Y, Hu Y, Huang L (2015) Graphene/$SrTiO_3$ nanocomposites used as an effective electron-transporting layer for high performance perovskite solar cells. RSC Adv 5:52041–52047
20. Rao CNR, Subrahmanyam KS, Ramakrishna Matte HSS, Maitra U, Moses K, Govindaraj A (2011) Graphene: synthesis, functionalization and properties. Int J of Modern Physics B 25:4107–4143
21. Zhang Y, Pan C (2011) TiO_2/graphene composite from thermal reaction of graphene oxide and its photocatalytic activity in visible light. J Mater Sci 46:2622–2626

22. Marcano DC, Kosynkin DV, Berlin JM (2010) Improved synthesis of graphene oxide. ACS Nano 4:4806–4814
23. Guo S, Dong S (2011) Graphene nanosheet: synthesis, molecular engineering, thin film, hybrids, and energy and analytical applications. Chem Soc Rev 40:2644–2672
24. Cihui L, Bingce L, Xi FZ (2008) Electrical and deep levels characteristics of ZnO/Si heterostructure by MOCVD deposition. Chi Phy B 17:172292
25. Chabane L, Zebbar N, Trari M, Kechouane M (2017) Opto-capacitive study of n-ZnO/p-Si heterojunctions elaborated by reactive sputtering method, Solar cell applications. Thin Solid Films 636:419–424
26. Bingce L, Cihui L, Bo Y (2010) Grain boundary layer behavior in ZnO/Si heterostructure. J Semicond 31
27. Lee C, Shin M, Lim M, Seo JY, Lee JE, Lee HY, Kim BJ, Choi D (2011) Material properties of microcrystalline silicon for solar cell application. Sol Energy Mater Solar Cells 95:207–210
28. Huang CH, Chuang WJ (2015) Dependence of performance parameters of CdTe solar cells on semiconductor properties studied by using SCAPS-1D. Vacuum 118:32–37
29. Adewoyin AD, Olopade MA, Oyebola OO, Chendo MA (2019) Development of CZTGS/CZTS tandem thin film solar cell using SCAPS-1D. Optik-Int J Light Electron Opt 176:132–142
30. Anwar F, Mahbub R, Satter SS, Ullah SM (2017) Effect of different HTM layers and electrical parameters on ZnO nanorod-based lead-free perovskite solar cell for high-efficiency performance. Int J Photoenergy 1–9
31. Mostefaoui M, Mayari H, Khelifi S, Bouraiou A, Dabou R (2015) Simulation of high efficiency CIGS solar cells with SCAPS-1D. Softw Energy Procedia 74:736–744
32. Minemoto T, Murat M (2014) Device modeling of perovskite solar cells based on structural similarity with thin film inorganic semiconductor solar cells. J Appl Phys 116
33. Lee DY, Na SI, Kim SS (2016) Graphene oxide/PEDOT:PSS composite hole transport layer for efficient and stable planar heterojunction perovskite solar cells. Nanoscale 8:1513–1522